THE PHYSICS OF THE HYPERFINE STRUCTURE IN THE HYDROGEN ATOM. THE HYDROGEN $\lambda = 21$ cm LINE

A. R. Kuzmak
Professor Ivan Vakarchuk Department for Theoretical Physics,
Ivan Franko National University of Lviv,
12, Drahomanov St., Lviv, UA-79005, Ukraine
e-mail: andrij.kuzmak@gmail.com

(Received 08 March 2024; in final form 03 May 2024; accepted 14 May 2024; published online 06 August 2024)

The paper provides a review and educational focus on the study of the hyperfine structure of the hydrogen atom, the exploration of which began in the middle of the last century. Since neutral hydrogen is the most common chemical element in the Universe, the radiation emitted due to the hyperfine splitting of its ground state allows for a wide observation of various astrophysical objects and the evolution of the Universe. Here, we describe the transition and calculate the average lifetime of the excited energy level within the hyperfine structure of the hydrogen atom. Additionally, we consider the influence of a magnetic field on the splitting and the average lifetime of the excited energy levels in this system.

Key words: hydrogen atom, hyperfine structure, the 21 cm line.

DOI: https://doi.org/10.30970/jps.28.3901

I. INTRODUCTION

The transition between energy levels, caused by the hyperfine splitting of the ground state of a neutral hydrogen atom, was theoretically predicted in 1944 by the Dutch astrophysicist Hendrik van de Hulst. Using quantum theory, he calculated the difference between the energy levels resulting from the splitting of the ground state of the hydrogen atom due to the interaction between the proton and electron spins [1–3]. This transition occurs through the absorption or emission of a photon with a wavelength of approximately 21 cm. The Earth's atmosphere is transparent to this radiation, allowing it to be observed by terrestrial observatories (for example, see [4]). Atomic hydrogen is a standard component of interstellar gas in galaxies, and in 1951, Harold Ewen and Edward Purcell first observed this line in our Galaxy [5]. Shortly afterward, astrophysicists from the Leiden Observatory, Jan Oort and C. A. Muller, as well as astrophysicists from Australia, W. N. Christiansen and J. V. Hindman, observed this line in our Galaxy as well [6, 7]. These observations enabled the construction of a map of neutral hydrogen for the first time, allowing the reproduction of the spiral structure of the Galaxy [8, 9]. More information about the experimental observation of the hydrogen line can be found in [10].

Analyzing the profile and intensity of the $\lambda = 21$ cm line allows for the determination of the temperature and density of the hydrogen cloud. Taking into account the Doppler broadening of the hydrogen line due to the movement of gas clouds, researchers measured the relative speed of rotation of the arms of our Galaxy [11]. This method has been instrumental in determining the structure and dynamics of various celestial objects. Observations of radiation from neutral hydrogen also enable the indirect estimation of galaxy masses [12]. The distribution of magnetic field strength within galaxies is determined by observing transitions between energy levels resulting from the Zeeman splitting of the ultrafine structure of this system [13].

Observing the hydrogen line is currently one of the few ways to probe into the 'dark ages', which began 380,000 years after the Big Bang (cosmological recombination) and lasted until the appearance of the first stars (for example, see [14–22]). This period corresponds to the redshift between $z = 1100$ (cosmological recombination) and $z = 30$ (appearance of the first stars and galaxies) [23, 24]. However, the transitions between the levels of the hyperfine structure become discernible after atomic hydrogen has sufficiently expanded and cooled. This moment corresponds to a redshift of $z \sim 100$ [24]. It is important to note that due to the redshift of the $\lambda = 21$ cm line, we observe radiation in the range from $\lambda = 1986$ cm ($\nu \approx 15$ MHz) to $\lambda = 652$ cm ($\nu \approx 46$ MHz). It is important to note that neutral hydrogen in the intergalactic space exists until the moment of reionization, which, according to observations, occurred at redshifts $z \sim 6 \ldots 8$. Therefore, the signal from the 21-cm line can be observed up to $\lambda = 147$ cm ($\nu \approx 204$ MHz).

Note that to date, only a single report has been published on the detection of an absorption profile in the sky-averaged radio spectrum in the 21 cm line of the early Universe centered at 78 MHz [25]. However, this result has been subject to ongoing critical evolution. Therefore, it can be stated that there has been still no reliable registration of signals in the 21 cm line from the early Universe. This is a matter of future observations.

Finally, we note that the wavelength and frequency of the hydrogen line were used to scale the images and time on the plates of the Pioneer, Voyager-1, and Voyager-2 spacecrafts [26]. On the Pioneer plate, the height of a woman is scaled as 8 wavelengths of $\lambda = 21$ cm, i. e., 168 cm (Fig. 1(a)). The Voyager plate depicts the location of the Sun relative to 14 pulsars and their rotation periods around their axis in units of hydrogen line

frequency (Fig. 1(b)). The 21 cm line also served as the theoretical basis for the search for extraterrestrial intelligence in the SETI program [27].

This paper provides a review and educational focus on the study of the hyperfine structure of the hydrogen atom. Since neutral hydrogen is the most common chemical element in the Universe (Sec II), the radiation emitted due to the hyperfine splitting of its ground state allows for a wide observation of various astrophysical objects and the evolution of the Universe. We describe the mechanism of splitting (Sec. III), transition energy (Sec. IV), and average lifetime of the excited energy level (Sec V) in the hyperfine structure of the hydrogen atom. Additionally, we consider the influence of the magnetic field on the energy levels (Sec. VI) and the wavelength of the radiation (Sec. VII) of this system. Finally, we briefly summarize the presented research in Sec. VIII.

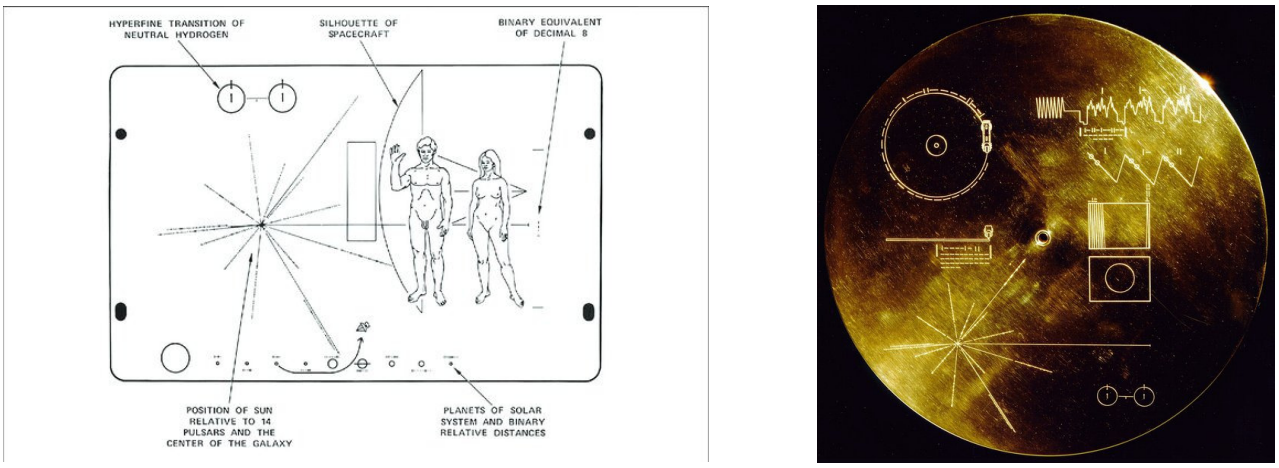

(a) (b)

Fig. 1. Pictures of the Pioneer (left figure), and Voyager (right figure) plates with images of a man and a woman, and the location of the Sun relative to 14 pulsars. Credit: NASA History

II. HYDROGEN IN THE UNIVERSE

Hydrogen is the lightest and most abundant chemical element, consisting of one proton and one electron. This isotope is designated as ^{1}H and is less commonly called protium. Hydrogen has a mass of 1.00782504(7) Da. Protons, which are the nuclei of hydrogen atoms, were formed within the first second after the Big Bang. After 380 000 years, when the temperature of the Universe dropped below the ionization temperature, electrons recombined with protons, leading to the formation of neutral hydrogen atoms. During the 'dark ages', protons accounted for 99.98% of the total number of atomic nuclei (for an example, see [22]). It is important to note that a small fraction (approximately 10^{-4}) of protons and electrons were scattered by the expansion of the Universe over great distances and could not recombine. Hydrogen constitutes 75% of the mass fraction relative to the total mass of matter in the Universe. Two hydrogen atoms can form a molecule that exists in a gaseous state. However, direct radiative association of two neutral hydrogen atoms in the ground states to form a hydrogen molecule is very unlikely. A catalyst is necessary for the formation of hydrogen molecules. Therefore, hydrogen gas in the early Universe mostly remains atomic. Hydrogen also has two isotopes: deuterium and tritium. Deuterium, denoted as ^{2}H, is a stable isotope with a nucleus consisting of one proton and one neutron. It has a mass of 2.013553212724(78) Da. The concentration of deuterium in ocean water is about 150 atoms per million hydrogen atoms, whereas after the Big Bang, the proportion of deuterium was 27 atoms per million hydrogen atoms. The tritium isotope, denoted as ^{3}H, consists of one proton and two neutrons, with a mass of 3.0160492 Da. It is unstable and decays into ^{3}He through the β-decay process with a half-life of 12.32 years. For instance, tritium is formed by the interaction of cosmic rays with gases in the upper atmosphere and during nuclear weapon explosions. It is also worth noting that other isotopes of hydrogen, namely ^{4}H, ^{5}H, ^{6}H, ^{7}H, have been synthesized in laboratory conditions. However, they are extremely unstable with very short half-lives on the order of $10^{-22} - 10^{-23}$ s. Information on the physical characteristics of various isotopes, including all isotopes of hydrogen, can be found in the paper [28]. Nevertheless, we will focus on the hydrogen atom ^{1}H, specifically on the transition between energy levels arising from the splitting of the ground state due to the interaction of the electron spin with the nuclear spin.

III. THE NATURE OF THE HYPERFINE STRUCTURE OF THE HYDROGEN ATOM

The hydrogen line (λ = 21 cm) arises as a result of the splitting of the ground state due to the interaction between the spins of the nucleus and the electron (Fig. 2). The nucleus of a hydrogen atom (proton) has a magnetic moment that creates a magnetic field, whi-

ch in turn affects the magnetic moment of an electron. The value of the magnetic field created by the magnetic moment of the proton $\mathbf{m}_\mathrm{p}$ at the distance $\mathbf{r}$ is well described in the dipole approximation (see Appendix A)

$$\mathbf{B} = \frac{\mu_0}{4\pi}\left(\frac{3\mathbf{r}\,(\mathbf{m}_\mathrm{p},\mathbf{r})}{r^5} - \frac{\mathbf{m}_\mathrm{p}}{r^3} + \frac{8\pi}{3}\mathbf{m}_\mathrm{p}\delta(\mathbf{r})\right), \qquad (1)$$

where μ_0 is the magnetic permeability of vacuum. The first two terms describe the magnetic field outside the dipole and the third term defines the magnetic field inside the dipole, respectively. The potential energy of the interaction between the magnetic field of the proton and the magnetic moment of the electron $\mathbf{m}_\mathrm{e}$ is given by the Hamiltonian

$$\mathbf{H} = -\,(\mathbf{m}_\mathrm{e},\mathbf{B})\,. \qquad (2)$$

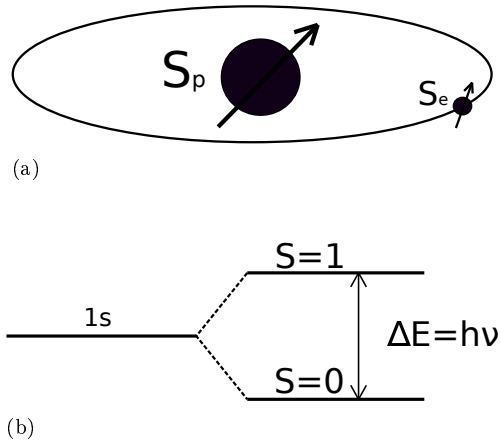

Fig. 2. The radiation of a hydrogen atom in the $\lambda = 21$ cm line is emitted due to the splitting of the ground state resulting from the interaction between the spins of the nucleus and the electron.

The spin-orbit interaction is not taken into account because we are considering the ground state of a hydrogen atom, in which its angular momentum is zero. However, in the case where the electron is at a higher energy level and possesses an angular momentum $\mathbf{L}$, it additionally interacts with the magnetic moment of the proton. In this scenario, an additional term should be added to the interaction energy, which takes the form $-\mu_0 e/(4\pi m_\mathrm{e} r^3)\,(\mathbf{L},\mathbf{m}_\mathrm{p})$, where e and m_e are the charge and mass of the electron, respectively. Note that the expression for potential energy (2) can be derived using the relation $\mathbf{F} = -\boldsymbol{\nabla} U$, where $\mathbf{F}$ is the force of interaction of two magnetic dipoles. For example, this derivation can be found in the textbook [29] (subsection 5.7). If we replace the coordinate variable and magnetic moments with operators in the Hamiltonian (2), we obtain a quantum mechanical Hamiltonian. The total Hamiltonian contains the kinetic energy operator of the electron and proton, as well as the potential energy of the Coulomb interaction. However, we are not interested in these terms because the interaction between the electron and proton spins is responsible for the splitting of the ground state (see, for example, textbooks [30–32]). These terms only result in a shift of the split energy levels relative to the energy of the ground state.

Let us express the Hamiltonian in terms of the interaction of magnetic moments. For this purpose, we average the Hamiltonian (2) over the wave function of the ground state, which has the following form

$$\psi_{1s}(r) = \frac{1}{\sqrt{\pi a_\mathrm{B}^3}} e^{-r/a_\mathrm{B}}, \qquad (3)$$

where $a_\mathrm{B} = \hbar^2/(m_\mathrm{e} e^2)$ is a 'Bohr radius'. Then, in the first order of the perturbation theory, the Hamiltonian takes the form

$$H = -\frac{\mu_0}{4\pi}\int \psi_{1s}^2(r)\left(\frac{3\,(\mathbf{m}_\mathrm{e},\mathbf{r})\,(\mathbf{m}_\mathrm{p},\mathbf{r})}{r^5} - \frac{(\mathbf{m}_\mathrm{e},\mathbf{m}_\mathrm{p})}{r^3} + \frac{8\pi}{3}\,(\mathbf{m}_\mathrm{e},\mathbf{m}_\mathrm{p})\,\delta(\mathbf{r})\right) dV. \qquad (4)$$

Using spherical coordinates with $\mathbf{r} = (r\sin\theta\cos\phi,\ r\sin\theta\sin\phi, r\cos\theta)$ and $dV = r^2\sin\theta\, dr\, d\theta\, d\phi$, and considering that the first two terms do not contribute to the region inside the dipole, we can easily verify that the integral of the first two terms in expression (4) with respect to the angle θ is equal to zero. Therefore, the Hamiltonian takes the form

$$H = -\frac{2\mu_0}{3}\psi_{1s}^2(0)\,(\mathbf{m}_\mathrm{e},\mathbf{m}_\mathrm{p}) = -\frac{2\mu_0}{3\pi a_\mathrm{B}^3}\,(\mathbf{m}_\mathrm{e},\mathbf{m}_\mathrm{p})\,. \qquad (5)$$

The proton and electron magnetic moment operators can be rewritten in terms of the spin operator as $\mathbf{m}_\mathrm{p} = \gamma_\mathrm{p}\mathbf{S}_\mathrm{p}$ and $\mathbf{m}_\mathrm{e} = \gamma_\mathrm{e}\mathbf{S}_\mathrm{p}$. Then, the Hamiltonian can be rewritten as follows

$$H = -\frac{2\mu_0\gamma_\mathrm{e}\gamma_\mathrm{p}}{3\pi a_\mathrm{B}^3}\,(\mathbf{S}_\mathrm{e},\mathbf{S}_\mathrm{p})\,, \qquad (6)$$

where $\gamma_{\mathrm{e(p)}} = e g_{\mathrm{e(p)}}/(2m_{\mathrm{e(p)}})$ is the gyromagnetic ratio of an electron (proton), $g_{\mathrm{e(p)}}$ is g-factor of the electron (proton), m_p is a mass of proton. The spin operator has the form

$$\mathbf{S}_{\mathrm{p(e)}} = \frac{\hbar}{2}\boldsymbol{\sigma}_{\mathrm{p(e)}} = \frac{\hbar}{2}\left(\sigma^x_{\mathrm{p(e)}}\mathbf{i} + \sigma^y_{\mathrm{p(e)}}\mathbf{j} + \sigma^z_{\mathrm{p(e)}}\mathbf{k}\right),$$

where

$$\sigma^x = \begin{pmatrix} 0 & 1 \\ 1 & 0 \end{pmatrix}, \quad \sigma^y = \begin{pmatrix} 0 & -i \\ i & 0 \end{pmatrix}, \quad \sigma^z = \begin{pmatrix} 1 & 0 \\ 0 & -1 \end{pmatrix} \qquad (7)$$

are the Pauli matrices. Finally, the Hamiltonian (6) takes the form

$$H = \frac{A}{4}\,(\boldsymbol{\sigma}_\mathrm{p},\boldsymbol{\sigma}_\mathrm{e})\,, \qquad (8)$$

where $A = -2\mu_0\gamma_\mathrm{e}\gamma_\mathrm{p}\hbar^2/(3\pi a_\mathrm{B}^3)$ represents the value of interaction between the spins of the nucleus and the electron of the hydrogen atom in the ground state. This interaction is isotropic and is described by the Heisenberg Hamiltonian. The difference between the energy levels of this Hamiltonian determines the energy splitting of the ground state.

IV. ENERGY LEVELS IN THE HYPERFINE STRUCTURE OF THE HYDROGEN ATOM

In this section, we determine the energy levels and eigenstates of the Hamiltonian (8) (see, for example, Appendix C in paper [33]). For this purpose, we express the Hamiltonian in the matrix representation. In the basis of the eigenstates of the operators $S_{\rm p}^z$ and $S_{\rm e}^z$, it takes the form

$$H = \begin{array}{c} \\ |\uparrow\uparrow\rangle \\ |\uparrow\downarrow\rangle \\ |\downarrow\uparrow\rangle \\ |\downarrow\downarrow\rangle \end{array} \begin{array}{c} \begin{array}{cccc} \langle\uparrow\uparrow| & \langle\uparrow\downarrow| & \langle\downarrow\uparrow| & \langle\downarrow\downarrow| \end{array} \\ \begin{pmatrix} \frac{A}{4} & 0 & 0 & 0 \\ 0 & -\frac{A}{4} & \frac{A}{2} & 0 \\ 0 & \frac{A}{2} & -\frac{A}{4} & 0 \\ 0 & 0 & 0 & \frac{A}{4} \end{pmatrix} \end{array}. \tag{9}$$

The energy levels E and eigenstates $|E\rangle$ of this Hamiltonian are determined from the equation

$$H|E\rangle = E|E\rangle. \tag{10}$$

Solving this equation, we obtain two energy levels with corresponding eigenstates

$$E_1 = -\frac{3}{4}A \ : \ |S\rangle = \frac{1}{\sqrt{2}}\left(|\uparrow\downarrow\rangle - |\downarrow\uparrow\rangle\right); \tag{11}$$

$$E_2 = \frac{1}{4}A \ : \ |T_1\rangle = |\uparrow\uparrow\rangle, \quad |T_2\rangle = \frac{1}{\sqrt{2}}\left(|\uparrow\downarrow\rangle + |\downarrow\uparrow\rangle\right), \quad |T_3\rangle = |\downarrow\downarrow\rangle, \tag{12}$$

where the first (second) state in the ket vectors corresponds to the spin state of the proton (electron). The states $|\uparrow\rangle$ and $|\downarrow\rangle$ represent positive and negative spin projections on the z axis, respectively. These are eigenstates of the z-component of the spin operator $\hbar\sigma^z/2$ with eigenvalues $\hbar/2$ and $-\hbar/2$, respectively. It is worth noting that this Hamiltonian is spherically symmetric, so the projections of eigenstates (11) and (12) onto an arbitrary direction are also eigenstates of this Hamiltonian. The ground state with energy E_1 is called a singlet because it corresponds to one eigenstate, and the excited level is called a triplet because it corresponds to three eigenstates. The total spin operator of the system $\mathbf{S} = \mathbf{S}_{\rm p} + \mathbf{S}_{\rm e}$ in the singlet state corresponds to the spin $S = 0$, while in the triplet state it corresponds to the spin $S = 1$. The difference between these energy levels is equal to the interaction energy of the nuclear spin with the electron spin as follows

$$\Delta E = E_2 - E_1 = A = -\frac{2\mu_0\gamma_{\rm e}\gamma_{\rm p}\hbar^2}{3\pi a_{\rm B}^3} \approx 9.4276\times10^{-25}\,{\rm J} \approx 5.8842\times10^{-6}\,{\rm eV}, \tag{13}$$

where $\gamma_{\rm e} = -1.76085963023\times10^{11}$ rad/(s · T), $\gamma_{\rm p} = 2.675221900\times10^{8}$ rad/(s · T) [34]. Given that $\Delta E = h\nu$, we can determine the frequency of the photon absorbed/emitted during such a transition as $\nu = \Delta E/h \approx 1\ 422.8$ MHz. The wavelength of this photon is $\lambda = c/\nu \approx 0.2107$ m = 21.07 cm, which corresponds to the decimeter range of electromagnetic radiation.

The observation of emitted or absorbed radiation during transitions between energy levels in the hyperfine structure of the hydrogen atom, measured in frequency units, yields the value $\nu = 1\ 420\ 405\ 751.767(773)$ Hz, corresponding to an energy of approximately $E \approx 9.4117\times10^{-25}$ J or $E \approx 5.8743\times10^{-6}$ eV. It can be observed that the theoretical value of the splitting of the ground state of a hydrogen atom obtained in this section due to the spin-spin interaction of a proton and an electron differs from the observed value by approximately 0.17%. This difference arises from the fact that we did not account for corrections from quantum electrodynamics, which include effects such as radiation effects, proton size, and vacuum polarization (see [35, 36] and references therein). It is noteworthy that Enrico Fermi was among the first to calculate corrections to the levels of atoms such as sodium (Na) and cesium (Cs) split into hyperfine structures [37]. Precise measurements of the hyperfine structure of the hydrogen atom were conducted in the 1970s by several laboratories, including the National Bureau of Standards (NBS) in the USA, the National Physical Laboratory (NPL) in the UK, the National Research Council of Canada (NRC), the Cesium-Based Navigation Signal System (LORAN C), the US Naval Observatory (USNO), the Paris Observatory Cesium Clock (TOP), and the French Atomic Clock (TAF) (see, for example, a review of the results in [38]).

The energy of the transition between levels E_1 (11) and E_2 (12) is quite small, and such a transition can occur due to the thermal motion of atoms at sufficiently low temperatures. The lowest temperature at which the energy transition in the hyperfine structure occurs can be estimated by equating the transition energy between levels (13) to the kinetic energy of two atoms moving towards each other, $\Delta E = k_{\rm B}T$. Consequently, we obtain the minimum excitation temperature for the transition as $T = h\nu/k_{\rm B} \approx 0.068$ K.

V. THE AVERAGE LIFETIME OF THE EXCITED STATE IN THE HYPERFINE STRUCTURE OF THE HYDROGEN ATOM

During the transition from the excited state to the ground state, the system emits a photon with energy $\hbar\omega = A$, wave vector $\mathbf{k}_0$, and polarization vector $\mathbf{e}_{\mathbf{k}_0,\alpha_0}$, where $\alpha_0 = 1,\ 2$ (indicating the two possible states of polarization for the photon). Since the excited state is threefold degenerate, any state from the triplet can be chosen for calculations. Let us select the state $|\uparrow\uparrow\rangle$. Then, considering the states of the electromagnetic field, the initial and final states of the system can be written as follows

$$|\psi_{\rm i}\rangle = |\psi_{1s}(r)\rangle|\uparrow\uparrow\rangle|0\rangle,$$

$$|\psi_{\rm f}\rangle = |\psi_{1s}(r)\rangle\frac{1}{\sqrt{2}}\left(|\uparrow\downarrow\rangle - |\downarrow\uparrow\rangle\right)|\gamma_{\mathbf{k}_0,\alpha_0}\rangle, \tag{14}$$

where $|0\rangle$ is the vacuum state of the photonic subsystem, and $|\gamma_{\mathbf{k}_0,\alpha_0}\rangle$ represents the state of the photonic subsystem containing a photon with wave vector $\mathbf{k}_0$ and polarization α_0. The interaction of the electron spin with the electromagnetic field is described by the Hamiltonian

$$H_{\rm int} = -\frac{g_{\rm e}e\hbar}{4m_{\rm e}c}\left(\boldsymbol{\sigma}_{\rm e},[\boldsymbol{\nabla},\mathbf{A}]\right) + \frac{e^2}{2m_{\rm e}c^2}\mathbf{A}^2, \qquad (15)$$

where the vector potential of the quantized magnetic field, which is located in a periodic cubic volume with sides L, has the form

$$\mathbf{A}(\mathbf{r}) = \sum_{\mathbf{k}}\sum_{\alpha=1,2}\sqrt{\frac{2\pi\hbar c^2}{ckL^3}}\mathbf{e}_{\mathbf{k},\alpha} \times \left(b_{\mathbf{k},\alpha}e^{i(\mathbf{k},\mathbf{r})} + b^{+}_{\mathbf{k},\alpha}e^{-i(\mathbf{k},\mathbf{r})}\right). \qquad (16)$$

Here, $b^{+}_{\mathbf{k},\alpha}$ and $b_{\mathbf{k},\alpha}$ are the creation and annihilation operators of a photon with wave vector $\mathbf{k}$ and polarization α. In Hamiltonian (15), we consider only the first term, which represents the first-order correction with respect to e. The second term represents a second-order correction, which we neglect. Considering (16), the Hamiltonian takes the form

$$H_{\rm int} = -\frac{g_{\rm e}e\hbar}{4m_{\rm e}c}i\sum_{\mathbf{k}}\sum_{\alpha=1,2}\sqrt{\frac{2\pi\hbar c^2}{ckL^3}}\left(\boldsymbol{\sigma}_{\rm e},[\mathbf{k},\mathbf{e}_{\mathbf{k},\alpha}]\right) \times \left(b_{\mathbf{k},\alpha}e^{i(\mathbf{k},\mathbf{r})} - b^{+}_{\mathbf{k},\alpha}e^{-i(\mathbf{k},\mathbf{r})}\right). \qquad (17)$$

The probability of transition per unit time from the state $|\psi_{\rm i}\rangle$ to the state $|\psi_{\rm f}\rangle$ under the influence of a disturbance described by Hamiltonian (17) is determined by Fermi's golden rule and is given by

$$\Gamma = \frac{2\pi}{c\hbar^2}\left(\frac{L}{2\pi}\right)^3\int_{\mathbf{k}}d\mathbf{k}\sum_{\alpha=1,2}\left|\langle\psi_{\rm f}|H_{\rm int}|\psi_{\rm i}\rangle\right|^2\delta(k_0-k), \qquad (18)$$

where $\delta(k_0-k)$ represents the Dirac delta function with an argument determined by the conservation law of energy. Here, we assume that the volume bounded by a cube with sides of length L is much larger than the dimensions of the system, allowing integration over k-space. In expression (18), we consider that the action of the annihilation operator on the vacuum state is equal to $b_{\mathbf{k},\alpha}|0\rangle = 0$, and the scalar product between two photon states is given by $\langle\gamma_{\mathbf{k}',\alpha'}|b^{+}_{\mathbf{k},\alpha}|0\rangle = \langle\gamma_{\mathbf{k}',\alpha'}|\gamma_{\mathbf{k},\alpha}\rangle = \delta_{\mathbf{k}',\mathbf{k}}\delta_{\alpha',\alpha}$. It is worth noting that at $\lambda = 0.21$ m and $r \approx a_{\rm B}$, we have $(\mathbf{k},\mathbf{r}) \approx 1.5\times10^{-9}$, and $\langle\psi_{1s}(r)|e^{-i(\mathbf{k},\mathbf{r})}|\psi_{1s}(r)\rangle = 1$. Therefore, the transition probability can be expressed as

$$\Gamma = \frac{\hbar}{2\pi c^2}\left(\frac{g_{\rm e}e}{4m_{\rm e}}\right)^2\int_{\mathbf{k}}d\mathbf{k}\,\frac{1}{k}\sum_{\alpha=1,2}\left|\frac{1}{\sqrt{2}}\left(\langle\uparrow\downarrow|-\langle\downarrow\uparrow|\right)\left(\boldsymbol{\sigma}_{\rm e},[\mathbf{k},\mathbf{e}_{\mathbf{k},\alpha}]\right)|\uparrow\uparrow\rangle\right|^2\delta(k_0-k). \qquad (19)$$

Let us rewrite the expression in spherical coordinates. Then, we obtain

$$\Gamma = \frac{\hbar}{2\pi c^2}\left(\frac{g_{\rm e}e}{4m_{\rm e}}\right)^2\int_0^{2\pi}d\phi\int_0^{\pi}k_0\sin\theta\,d\theta\sum_{\alpha=1,2}\left|\frac{1}{\sqrt{2}}\left(\langle\uparrow\downarrow|-\langle\downarrow\uparrow|\right)\left(\boldsymbol{\sigma}_{\rm e},[\mathbf{k},\mathbf{e}_{\mathbf{k},\alpha}]\right)|\uparrow\uparrow\rangle\right|^2. \qquad (20)$$

Photons emitted during the transition from the excited state to the ground state can propagate in any direction. Therefore, we write the wave vector in the form $\mathbf{k} = k_0(\sin\theta\cos\phi, \sin\theta\sin\phi, \cos\theta)$, and the two polarization vectors, which are orthogonal to each other and to the wave vector, take the form $\mathbf{e}_{\mathbf{k},1} = (\cos\theta\cos\phi, \cos\theta\sin\phi, -\sin\theta)$ and $\mathbf{e}_{\mathbf{k},2} = (-\sin\phi, \cos\phi, 0)$. Then, the triple products included in expression (20) are as follows

$$\begin{aligned}\left(\boldsymbol{\sigma}_{\rm e},[\mathbf{k},\mathbf{e}_{\mathbf{k},1}]\right) &= k_0\left(-\sigma^x_{\rm e}\sin\phi + \sigma^y_{\rm e}\cos\phi\right),\\ \left(\boldsymbol{\sigma}_{\rm e},[\mathbf{k},\mathbf{e}_{\mathbf{k},2}]\right) &= k_0\big(-\sigma^x_{\rm e}\cos\theta\cos\phi\\ &\quad - \sigma^y_{\rm e}\cos\theta\sin\phi + \sigma^z_{\rm e}\sin\theta\big).\end{aligned} \qquad (21)$$

Substituting these expressions into the formula for the transition probability (20), and after integration and simplification, we obtain

$$\begin{aligned}\Gamma &= \frac{\hbar}{2\pi c^2}\left(\frac{g_{\rm e}e}{4m_{\rm e}}\right)^2\frac{k_0^3}{2}\int_0^{2\pi}d\phi\int_0^{\pi}(1+\cos^2\theta)\sin\theta\,d\theta\\ &= \frac{\hbar g_{\rm e}^2e^2k_0^3}{12m_{\rm e}^2c^2}.\end{aligned} \qquad (22)$$

The average lifetime of the excited energy level is inversely proportional to the transition probability and has the form

$$\tau = \frac{1}{\Gamma} = \frac{12m_{\rm e}^2c^2}{\hbar g_{\rm e}^2e^2k_0^3}. \qquad (23)$$

Substituting the values of the quantities, and taking into account that $g_{\rm e} \approx -2$ and $k_0 = 2\pi/\lambda$, we find that the average lifetime of the excited state in the hyperfine structure of the hydrogen atom is approximately

$\tau \approx 3.4 \times 10^{14}$ s or 10^7 years. It is worth noting that in the SI system of units, the square of the electron charge e^2 should be multiplied by the electrostatic constant $1/(4\pi\epsilon_0)$, where ϵ_0 is the electric constant. The average lifetime of the excited state is on the order of 10 million years, indicating that the natural width of this line is very small. Such transitions are extremely rare, and in laboratory conditions, the intensity of such radiation is quite low. However, on the scale of the Universe, hydrogen is the most common element, so such a line is well-recorded in astrophysics.

VI. ENERGY LEVELS SPLITTING OF THE HYPERFINE STRUCTURE BY THE MAGNETIC FIELD

Let us examine the impact of the magnetic field on the energy levels of the hyperfine structure of the hydrogen atom. In this scenario, Hamiltonian (8) incorporates terms representing the interaction between proton and electron spins with the field. Because the spin interaction is isotropic, the field's direction does not alter the energy spectrum or the eigenstates of the system. Therefore, we select a coordinate system in which the field aligns with the positive direction of the z axis. The Hamiltonian of this system is expressed as

$$H = \frac{A}{4}\left(\boldsymbol{\sigma}_{\mathrm{p}}, \boldsymbol{\sigma}_{\mathrm{e}}\right) - \frac{\hbar\gamma_{\mathrm{p}}B}{2}\sigma_{\mathrm{p}}^{z} - \frac{\hbar\gamma_{\mathrm{e}}B}{2}\sigma_{\mathrm{e}}^{z}, \tag{24}$$

where B is the value of the magnetic field.

Similarly to the case without a magnetic field, we determine the eigenstates and eigenvalues of the system governed by Hamiltonian (24). The matrix representation of the Hamiltonian, includes additional terms with the magnetic field along the diagonal and has the form

$$H = \begin{array}{c} \\ |\uparrow\uparrow\rangle \\ |\uparrow\downarrow\rangle \\ |\downarrow\uparrow\rangle \\ |\downarrow\downarrow\rangle \end{array} \begin{array}{c} \begin{array}{cccc} \langle\uparrow\uparrow| & \langle\uparrow\downarrow| & \langle\downarrow\uparrow| & \langle\downarrow\downarrow| \end{array} \\ \begin{pmatrix} \frac{A}{4} - \frac{\hbar B}{2}(\gamma_{\mathrm{p}} + \gamma_{\mathrm{e}}) & 0 & 0 & 0 \\ 0 & -\frac{A}{4} - \frac{\hbar B}{2}(\gamma_{\mathrm{p}} - \gamma_{\mathrm{e}}) & \frac{A}{2} & 0 \\ 0 & \frac{A}{2} & -\frac{A}{4} + \frac{\hbar B}{2}(\gamma_{\mathrm{p}} - \gamma_{\mathrm{e}}) & 0 \\ 0 & 0 & 0 & \frac{A}{4} + \frac{\hbar B}{2}(\gamma_{\mathrm{p}} + \gamma_{\mathrm{e}}) \end{pmatrix} \end{array}. \tag{25}$$

The eigenvalues and eigenstates of this Hamiltonian are as follows

$$\begin{aligned} E_1 &= -\frac{A}{4} - \frac{1}{2}\sqrt{\hbar^2 B^2(\gamma_{\mathrm{p}} - \gamma_{\mathrm{e}})^2 + A^2}: && |S_{\mathrm{mf}}\rangle = -\sin\frac{\eta}{2}|\uparrow\downarrow\rangle + \cos\frac{\eta}{2}|\downarrow\uparrow\rangle; \\ E_2 &= \frac{A}{4} - \frac{\hbar B}{2}(\gamma_{\mathrm{p}} + \gamma_{\mathrm{e}}): && |T_{\mathrm{mf1}}\rangle = |\uparrow\uparrow\rangle; \\ E_3 &= -\frac{A}{4} + \frac{1}{2}\sqrt{\hbar^2 B^2(\gamma_{\mathrm{p}} - \gamma_{\mathrm{e}})^2 + A^2}: && |T_{\mathrm{mf2}}\rangle = \cos\frac{\eta}{2}|\uparrow\downarrow\rangle + \sin\frac{\eta}{2}|\downarrow\uparrow\rangle; \\ E_4 &= \frac{A}{4} + \frac{\hbar B}{2}(\gamma_{\mathrm{p}} + \gamma_{\mathrm{e}}): && |T_{\mathrm{mf3}}\rangle = |\downarrow\downarrow\rangle, \end{aligned} \tag{26}$$

where $\tan\eta = A/\left(\hbar B(\gamma_{\mathrm{p}} - \gamma_{\mathrm{e}})\right)$. As can be seen, the magnetic field splits the triplet state. Consequently, under the influence of a magnetic field, the triplet state spllits into three states. Figure 3 visually represents the gap between the energy levels of such a system based on the magnetic field. Since the proton's gyromagnetic ratio γ_{p} is three orders smaller than that of the electron γ_{e}, we disregard it. Recall that the electron's gyromagnetic ratio γ_{e} is negative, indicating that under the magnetic field's influence, E_2 splits in the positive energy direction, while E_4 assumes negative values.

By detecting the electromagnetic radiation formed due to transitions between the energy levels of the hyperfine structure of the hydrogen atom in a magnetic field (26), one can easily determine the magnitude of this field using the following expression:

$$E_i - E_j = \frac{2\pi\hbar c}{\lambda}, \tag{27}$$

where λ is the wavelength of the radiation.

It can be observed from Fig. 3 that at high magnetic fields, the dependence of the energy level splitting on the magnetic field behaves linearly. This is due to the fact that $(\hbar B\gamma_{\mathrm{e}})^2 \gg A^2$ and $\tan\eta = A/\left(\hbar B(\gamma_{\mathrm{p}} - \gamma_{\mathrm{e}})\right) \approx 0$ ($\sin\eta/2 \approx 0$, $\cos\eta/2 \approx 1$). In this scenario, the eigenvalues and eigenstates take the following form:

$$\begin{aligned} E_1 &= -\frac{A}{4} + \frac{\hbar B\gamma_{\mathrm{e}}}{2}: && |S_{\mathrm{mf}}\rangle = |\downarrow\uparrow\rangle \\ E_2 &= \frac{A}{4} - \frac{\hbar B\gamma_{\mathrm{e}}}{2}: && |T_{\mathrm{mf1}}\rangle = |\uparrow\uparrow\rangle, \\ E_3 &= -\frac{A}{4} - \frac{\hbar B\gamma_{\mathrm{e}}}{2}: && |T_{\mathrm{mf2}}\rangle = |\uparrow\downarrow\rangle, \\ E_4 &= \frac{A}{4} + \frac{\hbar B\gamma_{\mathrm{e}}}{2}: && |T_{\mathrm{mf3}}\rangle = |\downarrow\downarrow\rangle. \end{aligned} \tag{28}$$

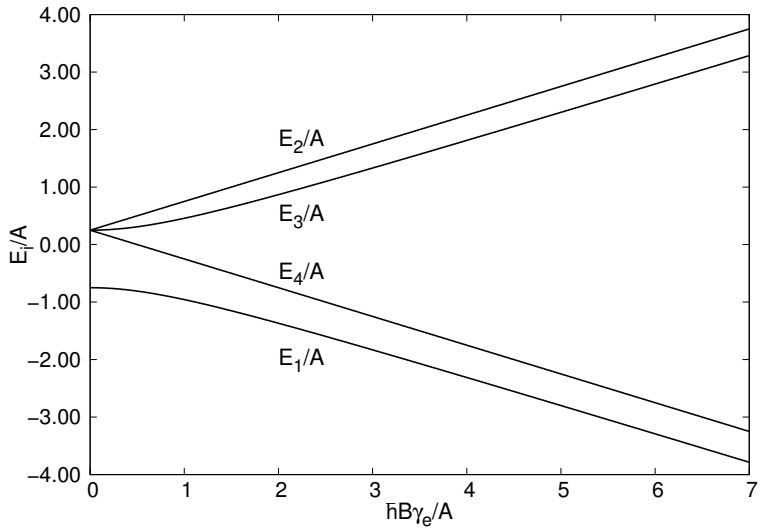

Fig. 3. Splitting of energy levels in the hyperfine structure of the hydrogen atom varies depending on the magnetic field. Since the gyromagnetic ratio of the electron γ_e is negative, the effect of the magnetic field causes E_2 to split in the positive energy direction, while E_4 takes on negative values.

Finally, we calculate the transition probabilities between the states (26). For this purpose, we substitute the states (26) into formula (20) with triple products (21). After performing the calculations, which were detailed in the previous section, we obtain the following transition probabilities for transitions between energy levels:

$$\begin{aligned}
\Gamma_{E_2\leftrightarrow E_1} &= \Gamma_{E_3\leftrightarrow E_4} = \frac{\hbar g_e^2 e^2 k_0^3}{6m_e^2c^2}\sin^2\frac{\eta}{2},\\
\Gamma_{E_3\leftrightarrow E_1} &= \frac{\hbar g_e^2 e^2 k_0^3}{12m_e^2c^2}4\sin^2\frac{\eta}{2}\cos^2\frac{\eta}{2},\\
\Gamma_{E_4\leftrightarrow E_1} &= \Gamma_{E_2\leftrightarrow E_3} = \frac{\hbar g_e^2 e^2 k_0^3}{6m_e^2c^2}\cos^2\frac{\eta}{2},\\
\Gamma_{E_2\leftrightarrow E_4} &= 0.
\end{aligned} \tag{29}$$

It is evident that the transition probabilities depend on the magnitude of the magnetic field, which is encapsulated in the η parameter. We recall that the wave number $k_0 = 2\pi/\lambda$ corresponds to the radiation emitted due to transition between the split levels, and $\lambda_{E_i\leftrightarrow E_j} = 2\pi\hbar c/(E_i - E_j)$. In a strong magnetic field, when $\sin(\eta/2) \approx 0$ and $\cos(\eta/2) \approx 1$, transitions $E_4 \leftrightarrow E_1$ and $E_2 \leftrightarrow E_3$ persist.

VII. THE WAVELENGTHS OF THE HYPERFINE STRUCTURE UNDER THE INFLUENCE OF MAGNETIC FIELDS IN THE UNIVERSE

In this section, we determine the wavelengths of the radiation that should be emitted during the transitions in the hyperfine structure of a hydrogen atom in a magnetic field. Given that the wavelength of the radiation generated by transitions between energy levels is equal to $\lambda_{E_i\leftrightarrow E_j} = 2\pi\hbar c/(E_i - E_j)$, we obtain

$$\begin{aligned}
\frac{\lambda_{E_2\leftrightarrow E_1}}{\lambda} &= 2\left(1 - \frac{\hbar B\gamma_e}{A} + \sqrt{1+\left(\frac{\hbar B\gamma_e}{A}\right)^2}\right)^{-1},\\
\frac{\lambda_{E_3\leftrightarrow E_1}}{\lambda} &= \left(1+\left(\frac{\hbar B\gamma_e}{A}\right)^2\right)^{-1/2},\\
\frac{\lambda_{E_4\leftrightarrow E_1}}{\lambda} &= 2\left(1 + \frac{\hbar B\gamma_e}{A} + \sqrt{1+\left(\frac{\hbar B\gamma_e}{A}\right)^2}\right)^{-1},\\
\frac{\lambda_{E_2\leftrightarrow E_3}}{\lambda} &= 2\left(1 - \frac{\hbar B\gamma_e}{A} - \sqrt{1+\left(\frac{\hbar B\gamma_e}{A}\right)^2}\right)^{-1},\\
\frac{\lambda_{E_3\leftrightarrow E_4}}{\lambda} &= 2\left(-1 - \frac{\hbar B\gamma_e}{A} + \sqrt{1+\left(\frac{\hbar B\gamma_e}{A}\right)^2}\right)^{-1}.
\end{aligned} \tag{30}$$

Here, we take into account that the wavelength of the hyperfine structure of a hydrogen atom in the absence of a magnetic field is $\lambda = 2\pi\hbar c/A$. It can be observed that the change in the wavelength of the radiation is determined by the value $\hbar\gamma_e B/A \approx -0.313\ \mathrm{T}^{-1} \times B$. In the case of the primary magnetic field that existed in the Universe during the 'dark ages', this value is on the order of $10^{-15} - 10^{-14}\times(1+z)^2$. This is because the magnitude of such a magnetic field is on the order of 10^{-13} T (1 nG) measured at the $z = 0$ [39]. To convert it to the redshift z, it the following relation $B(z) = B(0)(1+z)^2$ should be used. For detecting such radiation, it is necessary to take into account the redshift, as the radiation reaches us from distances determined by $z = 30-100$. The magnetic field inside galaxies varies from a few nT to several tens of nT [40]. Therefore, the value of $\hbar\gamma_e B/A$ should be in the range of $10^{-10} - 10^{-8}$.

VIII. CONCLUSIONS

Hydrogen is the most common chemical element in the Universe, the ground state of which is split into two due to the interaction between electron and proton spins. The nature of this splitting has been considered in detail, and such a system is described by the isotropic Heisenberg Hamiltonian with an interaction coupling equal to the difference between the energy levels. Using perturbation theory in the first order, these energy differences have been calculated. Consequently, the photon emitted or absorbed in such a transition has a wavelength close to 21 cm. Such a transition can occur due to the thermal motion of atoms at a sufficiently low temperature ($T \approx 0.068$ K). The average lifetime of the excited energy level has been calculated considering Fermi's Golden Rule, and it is equal to 10^7 years. Therefore, such transitions are very rare, and in laboratory conditions, the intensity of such radiation is quite low. However, on the scale of the Universe, hydrogen is the most common element, so this line is well recorded in astrophysics. It is worth noting that this line is currently one of the few ways to look into the 'dark ages'. Finally, we have considered the influence of the magnetic field on the splitting of the hyperfine structure of hydrogen atoms. We have shown how the difference between energy levels and their average lifetime depends on the magnetic field.

IX. ACKNOWLEDGMENTS

This work was supported by Project FF-27F (No. 0122U001558) from the Ministry of Education and Science of Ukraine.

Appendix A: Field from a magnetic dipole

In this appendix, we derive the vector potential and magnetic field from a magnetic dipole at a distant point. Similar calculations can be found in textbooks such as [3, 29, 41].

A.1. The vector potential is created by a magnetic dipole

A magnetic dipole can be represented by a circular conductor of radius a with a current I (Fig. 4). This conductor creates a magnetic moment $m = \pi a^2 I$, which is directed perpendicular to its plane according to the right-hand rule. We aim to calculate the intensity of the magnetic field $\mathbf{B}$ created by this conductor at any point P in space, which is far from the conductor at a distance much greater than its radius. For this purpose, we find the vector potential $\mathbf{A}$ that generates this field. Similar calculations can be found in textbooks such as [41]. Let us choose a coordinate system such that the conductor with current lies in the $x-y$ plane, the magnetic moment m is directed along the z axis, and the point P is above the x axis. In this case, the vector potential has two components in the $x-y$ plane. The definition of the vector potential is as follows:

$$\mathbf{A} = \frac{\mu_0 I}{4\pi} \oint_C \frac{d\mathbf{l}'}{r'}, \tag{A.1}$$

where μ_0 represents the magnetic permeability of vacuum, dl' represents a conductor element with current, and r' is the distance from this conductor element to point P. We set up the coordinate system such that this potential has two components located in the $x-y$ plane (see Fig. 4). Due to the circular symmetry of the conductor, the vector $d\mathbf{l}'$ can be rewritten in the form $d\mathbf{l}' = a(\sin\phi\mathbf{i} + \cos\phi\mathbf{j})d\phi$. Thus, the vector potential $\mathbf{A}$ is divided into two symmetrical components:

$$\mathbf{A} = \frac{\mu_0 I a}{4\pi} \int_0^{2\pi} \frac{\sin\phi}{r'} d\phi\mathbf{i} + \frac{\mu_0 I a}{4\pi} \int_0^{2\pi} \frac{\cos\phi}{r'} d\phi\mathbf{j}. \tag{A.2}$$

Let us rewrite r' through the angle ϕ. It can be seen from Fig. 4 that

$$r'^2 = r^2 + a^2 - 2ar\cos\chi. \tag{A.3}$$

It is also easy to see that

$$r\cos\chi = x\cos\phi. \tag{A.4}$$

Then

$$r' = \left(r^2 + a^2 - 2ax\cos\phi\right)^{1/2} = r\left(1 + \left(\frac{a^2}{r^2} - 2\frac{a}{r}\frac{x}{r}\cos\phi\right)\right)^{1/2}. \tag{A.5}$$

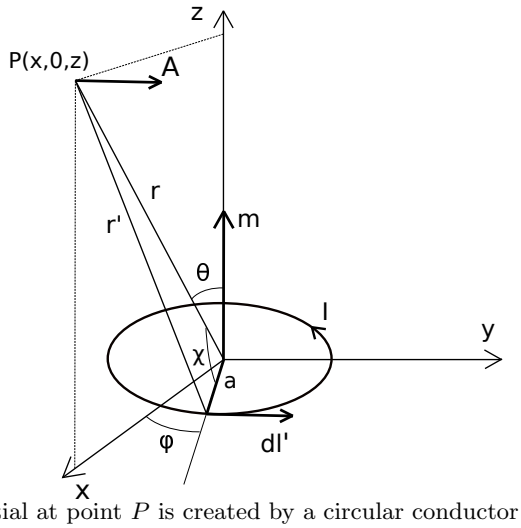

Figure 4. The vector potential at point P is created by a circular conductor of radius a with current I.

We examine the field at a distant point where $r \gg a$. It is also obvious that $x/r\cos\phi \leq 1$. Therefore, the expression in the brackets of equation (A.5) is small. Hence, we expand the expression $1/r'$ into a Taylor series, retaining terms from this brackets with an accuracy up to the second order as follows

$$\begin{aligned}\frac{1}{r'} &\approx \frac{1}{r}\left\{1-\frac{1}{2}\left(\frac{a^2}{r^2}-2\frac{a}{r}\frac{x}{r}\cos\phi\right)+\frac{3}{8}\left(\frac{a^2}{r^2}-2\frac{a}{r}\frac{x}{r}\cos\phi\right)^2\right\}\\ &= \frac{1}{r}\left\{1+\frac{a}{r}\frac{x}{r}\cos\phi-\left(\frac{1}{2}-\frac{3}{2}\frac{x^2}{r^2}\cos^2\phi\right)\frac{a^2}{r^2}-\frac{3}{2}\frac{a^3}{r^3}\frac{x}{r}\cos\phi+\frac{3}{8}\frac{a^4}{r^4}\right\}. \end{aligned} \tag{A.6}$$

Now, due to their smallness, we discard terms higher than a^2/r^2 from the expansion, yielding

$$\frac{1}{r'} \approx \frac{1}{r}\left\{1+\frac{a}{r}\frac{x}{r}\cos\phi-\left(\frac{1}{2}-\frac{3}{2}\frac{x^2}{r^2}\cos^2\phi\right)\frac{a^2}{r^2}\right\}. \tag{A.7}$$

Taking into account (A.7) in expression (A.2), the vector potential takes the form

$$\begin{aligned}\mathbf{A} &= \frac{\mu_0 Ia}{4\pi r}\left\{\left(1-\frac{a^2}{2r^2}\right)\int_0^{2\pi}(\sin\phi\mathbf{i}+\cos\phi\mathbf{j})\,d\phi\right.\\ &+ \left.\frac{ax}{r^2}\int_0^{2\pi}\left(\sin\phi\cos\phi\mathbf{i}+\cos^2\phi\mathbf{j}\right)d\phi+\frac{3a^2x^2}{2r^4}\int_0^{2\pi}\left(\cos^2\phi\sin\phi\mathbf{i}+\cos^3\phi\mathbf{j}\right)d\phi\right\}. \end{aligned} \tag{A.8}$$

Using trigonometric identities, we can easily verify that all integrals in this equation except the integral of $\cos^2\phi$ are equal to zero. Integral $\int_0^{2\pi}\cos^2\phi\,d\phi$ evaluates to π. Thus, we obtain the expression for the vector potential in the following form

$$\mathbf{A} = \frac{\mu_0 I\pi a^2 x}{4\pi r^3}\mathbf{j} = \frac{\mu_0 mx}{4\pi r^3}\mathbf{j}. \tag{A.9}$$

Here, we consider that $m = \pi a^2 I$ represents the magnetic moment arising from the conductor. The vector potential exhibits azimuthal symmetry. Considering that the magnetic moment is aligned along the z axis, we express equation (A.9) in the final form as follows

$$\mathbf{A} = \frac{\mu_0\,[\mathbf{m},\mathbf{r}]}{4\pi r^3}. \tag{A.10}$$

It is worth noting that a similar expression is obtained when the magnetic field is generated by any conductor with a current density $\mathbf{j}(\mathbf{r}_c)$. In this case, the magnetic moment takes the form

$$\mathbf{m} = \frac{1}{2}\int[\mathbf{r}_c,\mathbf{j}(\mathbf{r}_c)]\,d^3r_c. \tag{A.11}$$

Integration is performed over the entire volume of the conductor. Similar to the case of the ring, the distance to the point where the field is observed must be larger than the dimensions of the conductor. We do not delve into the detailed derivation, which can be found in the textbook [29].

Furthermore, if we consider the radius of the ring creating the magnetic moment as being compressed to an infinitely small ring, then any point outside this ring can be considered distant. The dipole formed in this manner can be interpreted as a point dipole. Equation (A.10) then describes the vector potential for such a dipole at any point in space. Let us now determine the magnetic field created by this dipole.

A.2. The magnetic field from a dipole

The magnetic field is determined from the vector potential as follows

$$\mathbf{B} = [\boldsymbol{\nabla}, \mathbf{A}]\,. \tag{A.12}$$

Substituting the expression for the vector potential of the dipole (A.10) in this equation, we obtain

$$\mathbf{B} = \frac{\mu_0}{4\pi}\left[\boldsymbol{\nabla}, \frac{[\mathbf{m}, \mathbf{r}]}{r^3}\right] = \frac{\mu_0}{4\pi}\left(\mathbf{m}\left(\boldsymbol{\nabla}, \frac{\mathbf{r}}{r^3}\right) - (\mathbf{m}, \boldsymbol{\nabla})\,\frac{\mathbf{r}}{r^3}\right). \tag{A.13}$$

From the Poisson equation

$$\Delta\frac{1}{r} = (\boldsymbol{\nabla}, \boldsymbol{\nabla})\,\frac{1}{r} = -\left(\boldsymbol{\nabla}, \frac{\mathbf{r}}{r^3}\right) = -4\pi\delta(\mathbf{r}) \tag{A.14}$$

we obtain that the field from the first term exists only inside of the dipole

$$\left(\boldsymbol{\nabla}, \frac{\mathbf{r}}{r^3}\right) = 4\pi\delta(\mathbf{r}). \tag{A.15}$$

The second term can be written as follows

$$(\mathbf{m}, \boldsymbol{\nabla})\,\frac{\mathbf{r}}{r^3} = \frac{1}{r^3}\,(\mathbf{m}, \boldsymbol{\nabla})\,\mathbf{r} + \mathbf{r}\left(\mathbf{m}, \boldsymbol{\nabla}\frac{1}{r^3}\right) + (\mathbf{m}, \boldsymbol{\nabla})\,\frac{\mathbf{r}}{r^3}\Big|_{\text{in}}\,, \tag{A.16}$$

where the first two terms describe the magnetic field outside the dipole, and the last one inside the dipole. It is easy to verify that the first two terms have the following form

$$\frac{1}{r^3}\,(\mathbf{m}, \boldsymbol{\nabla})\,\mathbf{r} + \mathbf{r}\left(\mathbf{m}, \boldsymbol{\nabla}\frac{1}{r^3}\right) = \frac{\mathbf{m}}{r^3} - \frac{3\mathbf{r}\,(\mathbf{m}, \mathbf{r})}{r^5}. \tag{A.17}$$

We study the field inside of the dipole as follows. We multiply the field vector $\mathbf{B}$ by an arbitrary vector $\mathbf{a}$ and integrate over the volume, which is a sphere of radius $\mathbf{r}$

$$\int_V (\mathbf{B}, \mathbf{a})\,dV = -\frac{\mu_0}{4\pi}\int_V (\mathbf{m}, \boldsymbol{\nabla})\left(\boldsymbol{\nabla}\frac{1}{r}, \mathbf{a}\right)dV = -\frac{\mu_0}{4\pi}\int_V \left(\mathbf{a}, (\mathbf{m}, \boldsymbol{\nabla})\,\boldsymbol{\nabla}\frac{1}{r}\right)dV, \tag{A.18}$$

where we use the identity $\boldsymbol{\nabla}\frac{1}{r} = -\frac{\mathbf{r}}{r^3}$. Taking into account that

$$(\mathbf{m}, \boldsymbol{\nabla})\,\boldsymbol{\nabla}\frac{1}{r} = \boldsymbol{\nabla}\left(\mathbf{m}, \boldsymbol{\nabla}\frac{1}{r}\right), \tag{A.19}$$

we rewrite (A.18) in the form

$$\int_V (\mathbf{B}, \mathbf{a})\,dV = -\frac{\mu_0}{4\pi}\int_V \left(\boldsymbol{\nabla}, \mathbf{a}\left(\mathbf{m}, \boldsymbol{\nabla}\frac{1}{r}\right)\right)dV = -\oint_S \left(\mathbf{a}\left(\mathbf{m}, \boldsymbol{\nabla}\frac{1}{r}\right), d\mathbf{S}\right), \tag{A.20}$$

where S is the area of the sphere bounding the volume V. Now substituting the explicit form of the gradient and taking into account that $d\mathbf{S} = r^2\mathbf{n}\,d\Omega$, where $\mathbf{n} = \mathbf{r}/r$ is a unit vector, and Ω is the solid angle, our integral takes the form

$$\int_V (\mathbf{B}, \mathbf{a})\,dV = \oint_S (\mathbf{a}, \mathbf{n}\,(\mathbf{m}, \mathbf{n}))\,d\Omega. \tag{A.21}$$

In the spherical coordinates $\theta \in [0, \pi]$, $\phi \in [0, 2\pi]$, vector $\mathbf{n}$ has the form $\mathbf{n} = (\sin\theta\cos\phi, \sin\theta\sin\phi, \cos\theta)$, $d\Omega = \sin\theta d\theta d\phi$. After integration, we obtain

$$\int_V (\mathbf{B}, \mathbf{a})\, dV = \frac{\mu_0}{3} (\mathbf{a}, \mathbf{m}) . \tag{A.22}$$

It is easy to see that such a result can be obtained when

$$\mathbf{B} = \frac{\mu_0}{3} \mathbf{m} \delta(\mathbf{r}) \tag{A.23}$$

or

$$(\mathbf{m}, \boldsymbol{\nabla}) \frac{\mathbf{r}}{r^3}\Big|_{in} = \frac{4\pi}{3} \mathbf{m} \delta(\mathbf{r}). \tag{A.24}$$

Substituting expressions (A.15) and (A.16) with (A.17), (A.24) into expression (A.13), we obtain the expression defining the magnetic field, which is created by a magnetic dipole

$$\mathbf{B} = \frac{\mu_0}{4\pi} \left(\frac{3\mathbf{r}\,(\mathbf{m}, \mathbf{r})}{r^5} - \frac{\mathbf{m}}{r^3} + \frac{8\pi}{3} \mathbf{m} \delta(\mathbf{r}) \right) . \tag{A.25}$$

Note that the first two terms describe the magnetic field outside the dipole, while the third term describes the magnetic field inside the dipole.

[1] D. J. Griffiths, Am. J. Phys. **50**, 698 (1982); https://doi.org/10.1119/1.12733.

[2] J. Gómez Subils, *Hyperfine Structure in Hydrogen: The 21 cm Line* (Universitat de Barcelona, 2015); http://hdl.handle.net/2445/67394.

[3] P. Maneekhum, Bachelor of Science in Physics thesis (Department of Physics, Faculty of Science Naresuan University, 2009); https://www.if.nu.ac.th/wp-content/uploads/2022/02/BS_thesisphatchaya.pdf.

[4] *American Practical Navigator: An Epitome of Navigation*, originally by N. Bowditch, LL.D (National Geospatial-Intelligence Agency, Springfield, VA, 2017), Vol. 1, Chap. 21; https://thenauticalalmanac.com/2017_Bowditch-_American_Practical_Navigator.html.

[5] H. I. Ewen, E. M. Purcell, Nature **168**, 356 (1951); https://doi.org/10.4236/wsn.2010.24048.

[6] C. Muller, J. Oort, Nature **168**, 357 (1951); https://doi.org/10.1038/168357a0.

[7] W. N. Christiansen, J. V. Hindman, Aust. J. Chem. **5**, 437 (1952); https://doi.org/10.1071/CH9520437.

[8] H. C. van de Hulst, C. A. Muller, J. H. Oort, Bull. Astron. Inst. Neth. **12**, 117 (1954).

[9] G. Westerhout, Bull. Astron. Inst. Neth. **13**, 201 (1957).

[10] E. M. Purcell, Proc. Am. Acad. Arts Sci. **82**, 347 (1953); https://doi.org/10.2307/20023736.

[11] F. J. Kerr, Ann. Rev. Astron. Astrophys. **7**, 39 (1969); https://doi.org/10.1146/annurev.aa.07.090169.000351.

[12] M. S. Roberts, S. Morton, Astron. J. **74** 859 (1969).

[13] G. L. Verschuur, Phys. Rev. Lett. **21**, 775 (1968); https://doi.org/10.1103/PhysRevLett.21.775.

[14] K. Kohler, N. Y. Gnedin, J. Miralda-Escude, P. A. Shaver, Astron. J. **633**, 552 (2005); https://doi.org/10.1086/444370.

[15] G. Mellema, I. T. Iliev, Ue-Li Pen, P. R. Shapiro, Mon. Not. R. Astron. Soc. **372**, 679 (2006); https://doi.org/10.1111/j.1365-2966.2006.10919.x

[16] J. R. Pritchard, A. Loeb, Rep. Prog. Phys. **75**, 086901 (2012); https://doi.org/10.1088/0034-4885/75/8/086901.

[17] A. Fialkov, A. Loeb, J. Cosmol. Astropart. Phys. **11**, 066 (2013); https://doi.org/10.1088/1475-7516/2013/11/066.

[18] S. R. Furlanetto, S. P. Oh, F. M. Briggs, Phys. Rep. **433**, 181 (2006); https://doi.org/10.1016/j.physrep.2006.08.002.

[19] J. R. Pritchard, A. Loeb, Phys. Rev. D **78**, 103511 (2008); https://doi.org/10.1103/PhysRevD.78.103511.

[20] J. O. Burns, Phil. Trans. R. Soc. A **379**, 20190564 (2021); https://doi.org/10.1098/rsta.2019.0564.

[21] B. Novosyadlyj, V. Shulga Yu., Kulinich, W. Han, Phys. Dark Universe **27**, 100422 (2020); https://doi.org/10.1016/j.dark.2019.100422.

[22] B. Novosyadlyj, Yu. Kulinich, G. Milinevsky, V. Shulga, Mon. Not. R. Astron. Soc. **526**, 2724 (2023); https://doi.org/10.1093/mnras/stad2927.

[23] J. Miralda-Escude, Science **300**, 1904 (2023); https://doi.org/10.1126/science.1085325.

[24] W. M. Peters, T. J. W. Lazio, T. E. Clarke, W. C. Erickson, N. E. Kassim, Astron. Astrophys. **525**, A128 (2011); https://doi.org/10.1051/0004-6361/201014707.

[25] J. D. Bowman, A. E. E. Rogers, R. A. Monsalve, Th. J. Mozdzen, N. Mahesh, Nature **555**, 67 (2018); https://doi.org/10.1038/nature25792.

[26] K. A. Capova, Front. Hum. Dyn. **3**, 714616 (2021); https://doi.org/10.3389/fhumd.2021.714616.

[27] G. Basalla, *Civilized Life in the Universe* (Oxford University Press, Oxford, 2006).

[28] F. G. Kondev, M. Wang, W. J. Huang, S. Naimi, G. Audi, Chin. Phys. C **45**, 030001 (2021); https://doi.org/10.1088/1674-1137/abddae.

[29] J. D. Jackson, *Classical Electrodynamics*, 3d ed. (John Wiley & Sons Inc., New York, 1998).

[30] A. Messiah, *Quantum Mechanics* (Dover Publication Inc, Mineola, New York, 1999).
[31] O. S. Davydov, *Quantum Mechanics* (Academy Periodyka, Kyiv, 2012) [in Ukrainian].
[32] I. O. Vakarchuk, *Quantum Mechanics* (Ivan Franko Lviv National University, Lviv, 2012) [in Ukrainian].
[33] J. A. Weil, J. R. Bolton, *Electron Paramagnetic Resonance: Elementary Theory and Practical Applications* (John Wiley & Sons, 2006); https://doi.org/10.1002/0470084987.
[34] *The NIST Reference on Constants, Units, and Uncertainty.* https://physics.nist.gov/cuu/Constants/index.html.
[35] S. J. Brodsky, G. W. Erickson, Phys. Rev. **148**, 26 (1966); https://doi.org/10.1103/PhysRev.148.26.
[36] S. J. Brodsky, S. D. Drell, Ann. Rev. Nucl. Sci. **20**, 147 (1970); https://doi.org/10.1146/annurev.ns.20.120170.001051.
[37] E. Fermi, Z. Phys. **60**, 320 (1930); https://doi.org/10.1007/BF01339933.
[38] S. G. Karshenboim, Can. J. Phys. 78, 639 (2000); https://doi.org/10.1139/p00-045.
[39] [Planck Collab.], Astron. Astrophys. **594**, A19 (2016); https://doi.org/10.1051/0004-6361/201525821.
[40] R. Beck, in: *How does the Galaxy Work?*, edited by E. J. Alfaro, E. Perez, J. Franco [Astrophysics and Space Science Library, Vol. 315] (Springer, Dordrecht, 2004).
[41] P. Lorrain, D. Corson, F. Lorrain, *Electromagnetic Fields and Waves*, 3rd ed. (W. H. Freeman and Company, New York, 1987).

ПРИРОДА НАДТОНКОЇ СТРУКТУРИ АТОМА ВОДНЮ. РАДІОЛІНІЯ ВОДНЮ $\lambda = 21$ см

А. Р. Кузьмак
Львівський національний університет імені Івана Франка,
кафедра теоретичної фізики імені професора Івана Вакарчука,
вул. Драгоманова, 12, Львів, 79005, Україна

Стаття має оглядовий та освітній характер щодо вивчення надтонкої структури атома водню, дослідження якої почалося в середині минулого століття. Оскільки нейтральний водень є найпоширенішим хімічним елементом у Всесвіті, випромінювання, що виникає внаслідок надтонкого розщеплення його основного стану, дає змогу широко спостерігати різноманітні астрофізичні об'єкти та еволюцію Всесвіту. У статті ми описуємо перехід між енергетичними рівнями та розраховуємо середній час життя збудженого стану в надтонкій структурі атома водню. Додатково ми розглядаємо вплив магнітного поля на розщеплення та середній час життя енергетичних рівнів у цій системі.

Ключові слова: атом водню, надтонка структура, радіолінія водню 21 см.